European Journal of Radiology 120 (2019) 108642

Contents lists available at ScienceDirect

European Journal of Radiology

journal homepage: www.elsevier.com/locate/ejrad

Research article

Analysis of heterogeneity of peritumoral T2 hyperintensity in patients with pretreatment glioblastoma: Prognostic value of MRI-based radiomics

Yangsean Choi, Kook-Jin Ahn*, Yoonho Nam, Jinhee Jang, Na-Young Shin, Hyun Seok Choi, So-Lyung Jung, Bum-soo Kim

Department of Radiology, Seoul St. Mary's Hospital, College of Medicine, The Catholic University of Korea, Republic of Korea

ARTICLE INFO

Keywords:
Glioblastoma
Radiomics
Texture analysis
MRI
Survival analysis

ABSTRACT

Purpose: On MR imaging, peritumoral T2 hyperintensity surrounding glioblastoma is known to contain tumor cell infiltrates, thus contributing to poor prognosis. This study aimed to determine the incremental prognostic value of radiomics on peritumoral T2 hyperintensity in pretreatment glioblastoma.

Methods: One hundred fourteen pathologically confirmed glioblastoma patients were retrospectively selected from March 2008 to May 2018 (our institution, n = 61; the Cancer Imaging Archive, n = 53). All patients were randomly divided into either training (n = 80) or test set (n = 34). Manually segmented peritumoral T2 hyperintensity yielded 106 radiomic features per patient. A random forest variable selection was used to select the most relevant radiomic features. Four Cox proportional hazards models were fitted with clinical features, clinical features with tumor/peritumoral volumes, radiomics, and all of them combined. Kaplan-Meier survival curves of the models were plotted with log-rank tests. All models were validated on a test set using prediction error curves over survival times.

Results: A random forest variable selection yielded five relevant features among the 106 radiomic features (two shape, two gray-level and one first order features). These radiomic features increased survival prediction accuracy when they were added onto clinical and tumor/peritumoral volumetric features (combined model, $P = 0.011$). On test set, the combined model showed lower mean survival prediction error rate (0.14) than clinical (0.191) or radiomic (0.178) model.

Conclusions: The clinical model with radiomic features demonstrated improved survival predictive performance than the model without radiomic features, thus suggesting incremental prognostic value of peritumoral radiomics as MR imaging biomarker in pretreatment glioblastoma.

1. Background

On MR imaging, peritumoral T2 hyperintensity is a common radiologic finding in glioblastoma—the most common primary malignant brain tumor in adults with a median overall survival (OS) of around 14.7 months [1]. Even with standard therapy of surgical resection followed by concurrent chemoradiation, the prognosis of glioblastoma remains dismally poor. After surgical resection, recurrences of glioblastoma usually occur along the resection margins where peritumoral hyperintensity is mixed; these recurrences proliferate more aggressively than the central glioblastoma cells [2,3], which adds difficulty for neurosurgeons in deciding the extent of surgical resection. Furthermore, the extent of peritumoral edema has been reported to contribute to poor prognosis [4]; however, the prognostic value of heterogeneity within peritumoral hyperintensity has not been established well. Therefore, understanding the significance of peritumoral T2 hyperintensity non-invasively on MR imaging would be meaningful for prognostic assessment. We assume that combining conventional clinical prognostic parameters with radiomics on peritumoral hyperintensity would improve survival prediction for patients initially diagnosed with glioblastoma.

Currently known clinical prognostic parameters of glioblastoma are age, KPS (Karnofsky performance score), extent of tumor resection, radio-chemotherapy, corticosteroid use, IDH1 and O6-methylguanine-DNA methyltransferase (MGMT) promoter methylation status [5–11]. In addition to such conventional parameters, many advances in imaging parameters have been made, one of which is radiomics—a field of quantitative extraction of subtle imaging features not easily discernible

* Corresponding author at: Department of Radiology, Seoul St. Mary's Hospital College of Medicine, The Catholic University of Korea, 222 Banpo-daero, Seocho-gu, Seoul, 06591, Republic of Korea.
E-mail address: ahn-kj@catholic.ac.kr (K.-J. Ahn).

https://doi.org/10.1016/j.ejrad.2019.108642
Received 19 March 2019; Received in revised form 1 August 2019; Accepted 18 August 2019

to radiologists and transforming them into minable data [12]. Texture features in describing patterns of heterogeneity of segmented brain tumors were reportedly linked to cellular anomalies within corresponding tissues [13]. Prior studies have found that conventional MR imaging characteristics [14] as well as texture [15,16] and radiomic features [17,18] extracted from enhancing, necrotic and non-enhancing edematous portions of glioblastoma were useful in predicting OS of patients. Compared to assessing enhancing portions alone, inclusion of T2-weighted images in assessing glioblastoma recurrence was found to improve progression-free survival prediction [19]. As for the predictive value of imaging, Pope et al [20] found that non-enhancing tumor, edema, satellites, and multifocality were significantly associated with prediction of survival. Particularly, non-enhancing peritumoral edema plays an important role in glioblastoma prognosis; severity of peritumoral edema at diagnosis is reportedly an independent negative prognostic factor [4,20,21]. In this regard, our work is designed to extend the radiomic analysis on peritumoral T2 hyperintensity in OS prediction. We hypothesized that radiomic analysis on non-enhancing peritumoral edema in addition to the conventional clinical prognostic parameters would improve OS prediction in patients with glioblastoma.

In this study, the performances of prognostic models constructed from clinical, radiomic and combined features will be evaluated. The present study aims to focus specifically on radiomic features' incremental prognostic value in survival prediction of glioblastoma patients.

2. Methods

2.1. Patient selection

Retrospective collection of clinical and imaging data was approved by the Institutional Review Board of our institution and informed consent was waived. Between March 2008 to May 2018, 203 patients diagnosed with glioblastoma at our institution were retrospectively selected. In addition, a separate cohort of 259 glioblastoma patients was collected from The Cancer Imaging Archive (TCIA) [22], an open archive of oncologic medical images. The inclusion criteria were 1) pathologically confirmed glioblastoma, 2) available pre-treatment MRI with conventional sequences [T2-weighted images (T2WI), T1-weighted images (T1WI), and contrast-enhanced T1-weighted images (T1CE)], 2) known survival status, and 3) clinical information (age, sex, type of surgical resection, MGMT promoter methylation status). 61 patients from our institution and 53 patients from TCIA met the above criteria giving a total study population of 114 patients.

2.2. Image acquisition

All pre-operative MRI were obtained on two 3.0 T MR scanners at our institution (Magnetom Verio; Siemens, Healthcare Sector, Erlangen, Germany) with a 12-channel phased-array coil and Ingenia (Philips Healthcare, Best, the Netherlands) with a 32-channel phased-array coil. Conventional sequences including T1WI, T1CE [echo time (TE): 3–4 ms; repetition time (TR): 8–10 ms), and T2 (TE: 140–150 ms; TR: 10–14 ms) were acquired. The scanning parameters were: 5-mm slice thickness, 250 × 250 mm^2 field of view and 256 × 256 pixel matrix. For TCIA dataset, either 1.5 T or 3.0 T MR scanners were used with sequences consisting of T1WI, T1CE [echo time (TE): 3–4 ms; repetition time (TR): 8–10 ms), and T2 (TE: 140–150 ms; TR: 10–14 ms). The scanning parameters were 5-mm slice thickness, 250 × 250 mm^2 field of view and 256 × 256 pixel matrix.

2.3. Image processing and segmentation

For each patient, peritumoral hyperintensity was manually segmented on T2WI by two neuroradiologists (BLINDED, BLINDED with 6 years and 20 years of experience, respectively). The T1CE and T2WI were co-registered after interscan motion corrections. Three-dimensional volume of interest covering the entire peritumoral hyperintensity was delineated by segmenting the region of interest (ROI) slice by slice on axial scans. Enhancing regions on T1CE as well as central solid and necrotic portions were subtracted from segmented images to selectively include the peritumoral hyperintensity. After additional reviewing session, any discrepancies in ROI were resolved by consensus. Morphologic features on MRI—tumor volume and peritumoral hyperintensity volume—were also assessed. All segmentations and registrations were carried out with NordicICE software (version 2.3.12, NordicNeuroLab AS, Bergen, Norway).

2.4. Radiomic feature extraction and selection

A publicly available python package Pyradiomics 2.1.0 [23] was used to extract radiomic features. One hundred six features consisting of grey level co-occurrence matrix (GLCM), grey-level run length matrix (GLRLM), grey-level size zone matrix (GLSZM), first-order, and shape features were extracted from peritumoral hyperintensity of T2WI. Since the number of parameters was greater than the number of patients in the test (n = 80) set, we used a random forest variable selection scheme with tree minimal depth methodology [24,25] to select a smaller subset of relevant features. The workflow of radiomics analysis is displayed in Supplementary Fig. 1.

2.5. Endpoints

The primary endpoint was OS of glioblastoma patients measured from the initial date of MR-based diagnosis to the death or last outpatient follow-up visit.

2.6. Statistical analysis

All statistical analyses were performed using R statistical and computing software (Version 3.3.1; http://www.r-project.org/). All patients were randomly grouped into a training and test set by 7:3 ratio (training set, n = 80; test set, n = 34) with balancing of survival status distribution between both groups. For this random dichotomization of cohort into training and test sets, 'caret' R package was used [26].

Continuous variables such as age, tumor volume and peritumoral hyperintensity volume were first tested for normality and then compared using Student's t test. Categorical variables including gender, MGMT methylation status and type of surgical resection were compared using x^2 test. To select the most relevant subset of radiomic features, 'randomForestSRC' R package was used. Four different models each fitted with a) clinical features (model 1), b) clinical features with tumor/peritumoral volumentric features (model 2), c) relevant subset of radiomic features (model 3), and d) all features combined (model 4) were created using multivariate Cox proportional hazards analyses. The Harrell's concordance index (C-index) for each model was computed to assess the survival predictive performance in the training set [27]. Moreover, analysis of deviance for different Cox regression models (ANOVA) was employed to determine whether the additive features (i.e. volumetric and radiomic features) improved the model fit from the clinical model. For assessment of overall performances of each model on test set, we used prediction error curves over survival time with the integrated Brier score via 'pec' R package [28].

Finally, 'survminer' R package was used to determine the optimal cutpoint for clinical and radiomic features, yielding maximal separation between high-risk and low-risk cohorts; Kaplan-Meier survival curves of the two risk groups were then plotted with log-rank tests for comparison of the curves. Statistical significance was set at $P < 0.05$. For comparison of model fits using ANOVA, statistical significance was set at $P < 0.025$ after Bonferroni correction. P-values of covariates within multivariate Cox regression models were adjusted using Benjamini & Hochberg correction [29].

Table 1
Clinical characteristics and tumor/peritumoral volumes of study population (n = 114).

Characteristic	Training group (n = 80)	Test group (n = 34)	*P* value
Age (years, mean ± SD)	57.4 ± 12.1	59.6 ± 12.5	0.383
Gender (n,%)			
Male	49 (61.3)	18 (52.9)	0.41
Female	31 (38.7)	16 (47.1)	
MGMT (n, %)			
Methylated	35 (43.8)	18 (52.9)	0.745
Unmethylated	45 (56.2)	16 (47.1)	
Type of surgical resection (n, %)			
Total	64 (80)	27 (79.4)	0.943
Subtotal/Partial	16 (20)	7 (20.6)	
Preoperative tumor volume (cm^3, mean ± SD)	27.5 ± 23.0	24.4 ± 20.7	0.436
Preoperative peritumoral hyperintensity volume (cm^3, mean ± SD)	50.5 ± 41.2	49.2 ± 42.2	0.957
Overall survival [days; mean (range)]	610 (82-2213)	623 (121-2125)	0.582

3. Results

3.1. Baseline characteristics of study population

The characteristics of training and test groups are summarized in Table 1. The training group consisted of 80 patients (49 males and 31 females; mean age, 57.4 ± 12.1 years) with mean OS of 610 days (range, 82–2213 days). The test group consisted of 34 patients (18 males, 16 females; mean age, 59.6 ± 12.5 years) with mean OS of 623 days (range, 121–2125 days). No significant differences were observed between both groups regarding age, gender, MGMT promoter methylation status, type of surgical resection, preoperative tumor volume/peritumoral hyperintensity area and OS (P = 0.383-0.957).

3.2. Model building using clinical and radiomics features

The Cox proportional hazards models fitted with clinical features (model 1), clinical features with volumetric features (model 2), radiomics (model 3), and all features (model 4) of the training set are shown in Table 2. Among the clinical variables, age was found to be a significant variable in the univariate Cox proportional hazards model (HR = 1.02; P = 0.027). The type of surgical resection showed borderline statistical significance (HR = 1.78; P = 0.051). Preoperative tumor volume and peritumoral hyperintensity volume were not found to be significant prognostic factors on univariate Cox proportional hazards analyses (P = 0.062 and P = 0.099, respectively). Model 1 was fitted with three clinical features (type of surgical resection, age, and MGMT promoter methylation status); model 2 was fitted with clinical features and tumor/peritumoral volumetric features. Model 3 was fitted with the five most relevant radiomic features—two shape features (elongation and sphericity), two gray-level co-occurrence matrix features (inverse difference normalized and inverse difference moment normalized), and one first-order feature (maximum intensity)—obtained via random forest variable selection (Supplemental Table 1). Finally, model 4 was fitted with all features (clinical, volumetric and radiomic features).

3.3. Survival predictive performances and model validation on testing set

The clinical, clinical with volumetric, radiomic and combined models had C-indices of 0.595 (P = 0.047), 0.664 (P = 0.007), 0.659 (P = 0.006), and 0.699 (P < 0.001), respectively. When volumetric and radiomic features were consecutively added onto the clinical model, the ANOVA showed increasing log-likelihood for each addition (P = 0.017 and P = 0.011, respectively) indicating improved model fit (Table 2). The Kaplan-Meier survival curves of high-risk and low-risk groups as stratified by the clinical model showed no significant difference (P = 0.71, Fig. 1a) while those stratified by the radiomic model showed significant difference (P < 0.006, Fig. 1b); the survival stratification by the combined model showed the greatest difference (P < 0.001, Fig. 1c). The risk prediction errors of the four models that were validated on the test set are shown in Fig. 2, and detailed prediction error rates (or integrated Brier scores) are displayed in Table 3. Overall, the combined model showed lowest mean prediction error rates (0.14) than any of the three model (range, 0.178-0.191). Representative images with peritumoral edema are shown in Fig. 3.

Table 2
(a) Univariate Cox regression analyses of clinical variables and tumor/peritumoral volumes. (b) Multivariate Cox regression models with ANOVA.

(a) Clinical variables and tumor/peritumoral volumes	HR	CI	Concordance index	P-value
Resection	1.78	1.00-3.17	0.554	0.051
Age	1.02	1.00-1.05	0.565	*0.027*
Sex	0.64	0.39-1.06	0.55	0.08
MGMT methylation status	0.67	0.41-1.09	0.536	0.104
Peritumoral hyperintensity volume[a]	1.49	0.927-2.41	0.577	0.099
Tumor volume[b]	0.51	0.253-1.035	0.547	0.062
(b) Four different Cox multivariate models[c] with ANOVA	Concordance index			P-value
Model 1	0.595			*0.047*
Model 2	0.664			*0.007*
Model 3[d]	0.659			*0.006*
Model 4[e]	0.699			*< 0.001*
ANOVA	Chi-square			P-value[f]
Model 1 vs. Model 2	8.12			*0.017*
Model 2 vs. Model 4	14.78			*0.011*

HR hazards ratio, *CI* 95% confidence interval, *ANOVA* analysis of deviance for different Cox regression models, *MGMT* O6-methylguanine-DNA methyltransferase.

[a] Volume threshold set at 37.5 cm^3.

[b] Volume threshold set at 7.8 cm^3.

[c] Model 1: age, resection and MGMT methylation status; model 2: model 1 + tumor/peritumoral volume; model 3: relevant radiomic features; model 4: all features.

[d] Adjusted P-values of five relevant radiomic features were all < 0.05 after Benjamini & Hochberg correction.

[e] Adjusted P-values of five relevant radiomic features and peritumoral hyperintensity volume were all < 0.05 after Benjamini & Hochberg correction.

[f] Statistical significance set at P < 0.025 after Bonferroni correction.

4. Discussion

The highly variable OS among glioblastoma patients associated with its aggressive clinical course has been attributed to its heterogeneous biological traits [30]. It is now widely believed that this infiltrative heterogeneity spreads beyond the tumoral margins and into the peritumoral brain zone [31,32], often manifested as T2 hyperintensity. This study demonstrates a high-throughput radiomic analysis on pretreatment peritumoral T2 hyperintensity of glioblastoma patients. In addition to assessing the conventional clinical variables, we applied quantitative radiomic analysis to construct both clinical and radiomic prognostic models. This is an important step forward to understanding the prognostic value of heterogeneity within peritumoral T2 hyperintensity of glioblastoma via radiomics, thereby allowing risk stratification of patients.

Of the clinical variables, only age showed statistical significance within the univariate Cox proportional hazards analysis, but we nonetheless included the type of surgical resection and MGMT promoter methylation status since they are very well-known prognostic

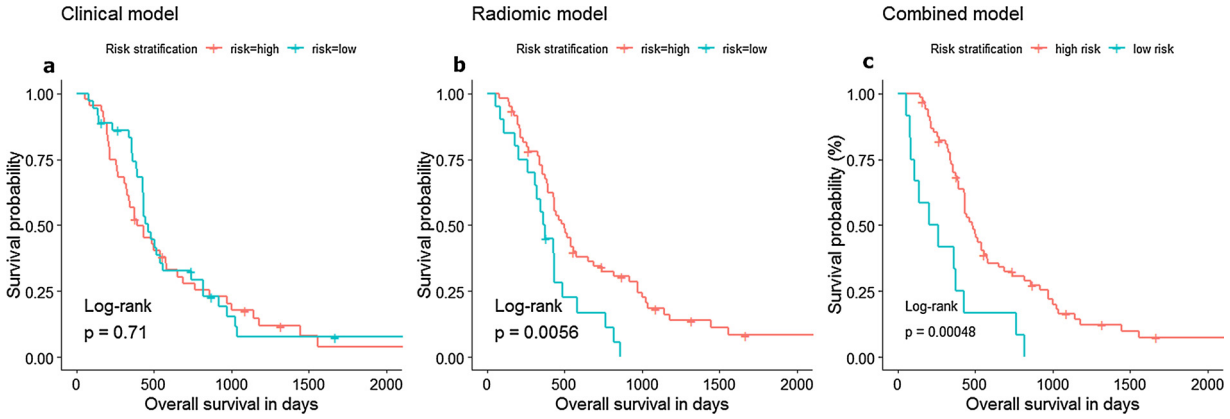

Fig. 1. Kaplan-Meier survival curves of the clinical (a), radiomic (b) and combined (c) models. The green and red lines indicate low-risk and high-risk patients, respectively.

parameters of glioblastoma [33,34]. The type of surgical resection, however, showed borderline statistical significance ($P = 0.051$) with a meaningful hazards ratio (HR: 1.78, CI: 1.00–3.17); these findings suggest that gross total resection yields more favorable prognosis than non-total resection, which is consistent to previous studies [34,35]. Both pretreatment tumor and peritumoral hyperintensity volumes were not associated with patients' OS. These findings were partially consistent with a previous study by Henker et al. [36] who demonstrated that tumor volume, but not the peritumoral edema volume, is significantly associated with survival. We assume that differences in measurement technique—their volumetric analysis was based on 3D segmentation—may be attributable to the conflicting findings. However, our findings were consistent with another study by Hammoud et al. [21] who showed that preoperative tumor volume was not a significant predictor of survival. Although tumor/peritumoral volumes were not significantly associated with survival, they improved the survival predictive performance when they were added onto the clinical model.

Regarding peritumoral edema, a previous study by Schoenegger et al. [4] showed that pretreatment peritumoral edema of glioblastoma on T2-weighted MRI was an independent prognostic factor. Their results demonstrated that patients with a larger area of peritumoral edema (> 1 cm from tumor margin) had significantly shorter OS. Another study, however, showed that association of extent of peritumoral edema to survival was inconclusive [37]. Our study attempted more

Table 3
Prediction performances on test set with integrated Brier scores.

		Integrated Brier scores[a] (prediction error rates)				
Overall survival (days)	No. at risk	Reference[b]	Model 1[c]	Model 2	Model 3	Model 4
328	26	0.148	0.133	0.146	0.141	0.114
473	18	0.241	0.234	0.229	0.2	0.182
732	9	0.218	0.206	0.183	0.192	0.124
Mean integrated Brier scores		0.202	0.191	0.186	0.178	0.14

[a] Lower integrated Brier scores indicate better predictive performance.
[b] Kaplan-Meier survival estimation.
[c] Model 1: age, resection and MGMT methylation status; model 2: model 1 + tumor/peritumoral volume; model 3: relevant radiomic features; model 4: all features.

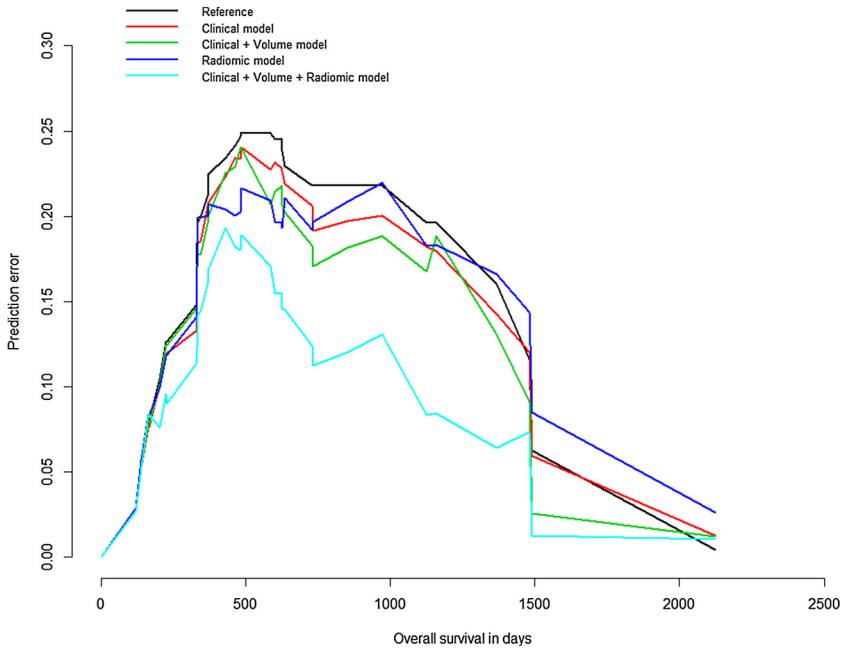

Fig. 2. Prediction error curves of the clinical (red), clinical with volume (green), radiomic (blue) and combined (light blue) models. Reference (black) indicates Kaplan-Meier survival estimation.

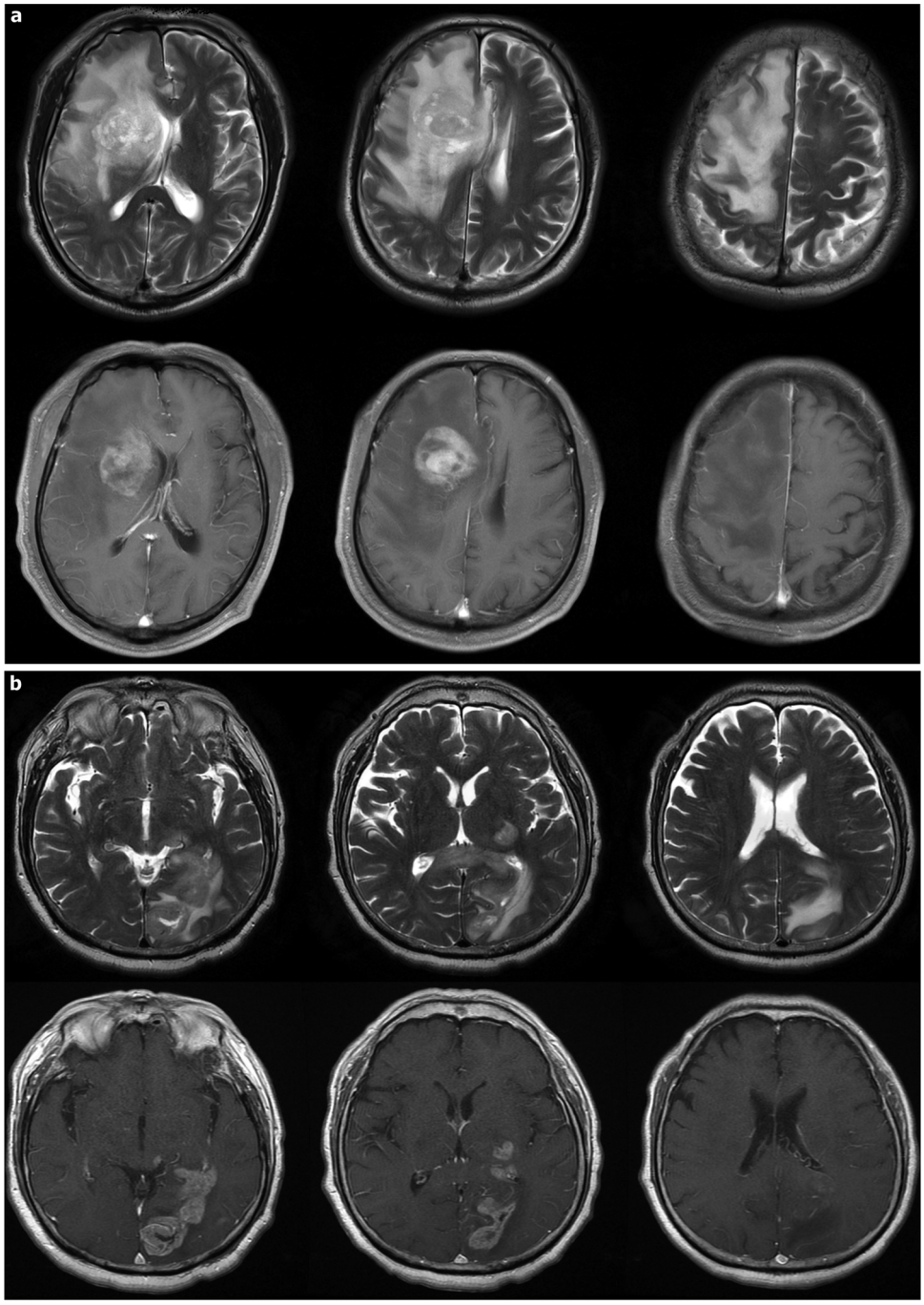

Fig. 3. Representative images of two patients with long (a) and short-term (b) overall survival (851 and 172 days, respectively). The first-order feature (maximum) was higher in long-term survivor (399.8 vs. 266) while the shape feature (elongation) was higher in the short-term survivor (0.71 vs. 0.58). Upper row: T2-weighted images; lower row: gadolinium-enhanced T1-weighted images.

computationally rigorous analysis on peritumoral T2 hyperintensity via radiomics approach, incorporating first-order, shape, and texture features, thereby overcoming previous studies' limitations on area and volumetric analyses. A similar study by Prasanna et al. [17] showed that radiomic features extracted from peritumoral edema on T2WI had a C-index of 0.637, which is comparable to our findings of 0.659. Furthermore, as seen in our findings, their study selected five most predictive radiomic features from peritumoral edema. Unlike their study, however, this study consisted of a larger cohort and an independent test cohort to validate our models.

The subset of 5 most relevant radiomic features (4.7% of the total features) were extracted solely from the non-enhancing portion of peritumoral T2 hyperintensity. The radiomic analysis based only on T2WI that are routinely acquired on conventional MR scans would allow wider applications in any setting where complex multi-parametric sequences are not available. Interestingly, two GLCM features were included in the subset of relevant features; these features capture underlying lesion heterogeneity and have been shown to predict aggressive growth and poor treatment response [17]. A previous study by Chaddad et al. [38] also found that a homogeneity radiomic feature computed from peritumoral edema regions was significantly associated with survival in patients with glioblastoma. We assume that these findings further imply the possible association between peritumoral heterogeneity with patients' survival. Moreover, the shape sphericity

feature reflecting asphericity (or shape irregularity) was one of the five radiomic features, which may suggest more irregular-shaped peritumoral hyperintensity was associated with poor outcome.

In both training and test cohorts, the combined model incorporating clinical, volumetric and radiomic features showed highest survival predictive performance than all other models, a finding consistent with Prasanna et al [17]. The internal validation of all four models via risk prediction error rates over survival time showed that radiomic model had a lower mean integrated Brier score than that of clinical model. The combined model, however, outperformed all the other models with lower integrated Brier scores in all time intervals (328–732 OS days). In addition, the prediction error rates of the combined model were prominently lowest during one to four years of survival period. This finding possibly suggests that radiomic features—with their potential incremental survival prognostic value—may yield the best prognostic performance over one to four years of survival period.

There are a few limitations to be addressed in this study. First, although our prognostic models were separately validated on a test set, their performance was not validated on an independent external cohort from a different institution, which is a more robust validation method. In addition, inclusion other well-known prognostic parameter such as IDH1 or Karnofsky performance score was not possible due to missing information. Correlation between prognostic genetic markers and radiomics—known as radiogenomics—would have strengthened our results. Furthermore, the variable acquisitions of MRI data limited us to analyze 2D scans only rather than 3D scans which could have added better delineation of ROI with possibly improved radiomic feature extraction. Finally, our study lacked progression-free survival because the images from TCIA did not contain information regarding progression as defined by RANO (Response Assessment in Neuro-Oncology) criteria.

In conclusion, radiomic features of peritumoral T2 hyperintensity combined with clinical and volumetric parameters provided improved OS prediction in pretreatment glioblastoma patients, suggesting the potential incremental prognostic value of radiomics as imaging biomarker.

Ethical approval

All procedures performed in studies involving human participants were in accordance with the ethical standards of the institutional and/or national research committee and with the 1964 Helsinki declaration and its later amendments or comparable ethical standards.

Informed consent

The institutional review board approved this retrospective study and informed consent was waived.

Funding

This research did not receive any specific grant from funding agencies in the public, commercial, or not-for-profit sectors.

Declaration of Competing Interest

The authors declare that they have no conflict of interest.

Appendix A. Supplementary data

Supplementary material related to this article can be found, in the online version, at doi:https://doi.org/10.1016/j.ejrad.2019.108642.

References

[1] R. Stupp, W.P. Mason, M.J. van den Bent, M. Weller, B. Fisher, M.J. Taphoorn, K. Belanger, A.A. Brandes, C. Marosi, U. Bogdahn, J. Curschmann, R.C. Janzer, S.K. Ludwin, T. Gorlia, A. Allgeier, D. Lacombe, J.G. Cairncross, E. Eisenhauer, R.O. Mirimanoff, R. European Organisation for, T. Treatment of Cancer Brain, G. Radiotherapy, G. National Cancer Institute of Canada Clinical Trials, Radiotherapy plus concomitant and adjuvant temozolomide for glioblastoma, N. Engl. J. Med. 352 (10) (2005) 987–996.

[2] P. Ruiz-Ontanon, J.L. Orgaz, B. Aldaz, A. Elosegui-Artola, J. Martino, M.T. Berciano, J.A. Montero, L. Grande, L. Nogueira, S. Diaz-Moralli, A. Esparis-Ogando, A. Vazquez-Barquero, M. Lafarga, A. Pandiella, M. Cascante, V. Segura, J.A. Martinez-Climent, V. Sanz-Moreno, J.L. Fernandez-Luna, Cellular plasticity confers migratory and invasive advantages to a population of glioblastoma-initiating cells that infiltrate peritumoral tissue, Stem Cells 31 (6) (2013) 1075–1085.

[3] M. Glas, B.H. Rath, M. Simon, R. Reinartz, A. Schramme, D. Trageser, R. Eisenreich, A. Leinhaas, M. Keller, H.U. Schildhaus, S. Garbe, B. Steinfarz, T. Pietsch, D.A. Steindler, J. Schramm, U. Herrlinger, O. Brustle, B. Scheffler, Residual tumor cells are unique cellular targets in glioblastoma, Ann. Neurol. 68 (2) (2010) 264–269.

[4] K. Schoenegger, S. Oberndorfer, B. Wuschitz, W. Struhal, J. Hainfellner, D. Prayer, H. Heinzl, H. Lahrmann, C. Marosi, W. Grisold, Peritumoral edema on MRI at initial diagnosis: an independent prognostic factor for glioblastoma? Eur. J. Neurol. 16 (7) (2009) 874–878.

[5] J.C. Buckner, Factors influencing survival in high-grade gliomas, Semin. Oncol. 30 (6 Suppl 19) (2003) 10–14.

[6] K.A. Carson, S.A. Grossman, J.D. Fisher, E.G. Shaw, Prognostic factors for survival in adult patients with recurrent glioma enrolled onto the new approaches to brain tumor therapy CNS consortium phase I and II clinical trials, J. Clin. Oncol. 25 (18) (2007) 2601–2606.

[7] M. Lacroix, D. Abi-Said, D.R. Fourney, Z.L. Gokaslan, W. Shi, F. DeMonte, F.F. Lang, I.E. McCutcheon, S.J. Hassenbusch, E. Holland, K. Hess, C. Michael, D. Miller, R. Sawaya, A multivariate analysis of 416 patients with glioblastoma multiforme: prognosis, extent of resection, and survival, J. Neurosurg. 95 (2) (2001) 190–198.

[8] A.M. Stark, A. Nabavi, H.M. Mehdorn, U. Blomer, Glioblastoma multiforme-report of 267 cases treated at a single institution, Surg. Neurol. 63 (2) (2005) 162–169 discussion 169.

[9] W. Stummer, H.J. Reulen, T. Meinel, U. Pichlmeier, W. Schumacher, J.C. Tonn, V. Rohde, F. Oppel, B. Turowski, C. Woiciechowsky, K. Franz, T. Pietsch, A.L.-G.S. Group, Extent of resection and survival in glioblastoma multiforme: identification of and adjustment for bias, Neurosurgery 62 (3) (2008) 564–576 discussion 564-76.

[10] C. Hill, S.B. Hunter, D.J. Brat, Genetic markers in glioblastoma: prognostic significance and future therapeutic implications, Adv. Anat. Pathol. 10 (4) (2003) 212–217.

[11] radiol.2016151913.pdf.

[12] R.J. Gillies, P.E. Kinahan, H. Hricak, Radiomics: images are more than pictures, they are data, Radiology 278 (2) (2016) 563–577.

[13] J. Lee, R. Jain, K. Khalil, B. Griffith, R. Bosca, G. Rao, A. Rao, Texture feature ratios from relative CBV maps of perfusion MRI are associated with patient survival in glioblastoma, AJNR Am. J. Neuroradiol. 37 (1) (2016) 37–43.

[14] K. Wang, Y. Wang, X. Fan, J. Wang, G. Li, J. Ma, J. Ma, T. Jiang, J. Dai, Radiological features combined with IDH1 status for predicting the survival outcome of glioblastoma patients, Neuro Oncol. 18 (4) (2016) 589–597.

[15] A. Chaddad, C. Tanougast, Extracted magnetic resonance texture features discriminate between phenotypes and are associated with overall survival in glioblastoma multiforme patients, Med. Biol. Eng. Comput. 54 (11) (2016) 1707–1718.

[16] O. Gevaert, L.A. Mitchell, A.S. Achrol, J. Xu, S. Echegaray, G.K. Steinberg, S.H. Cheshier, S. Napel, G. Zaharchuk, S.K. Plevritis, Glioblastoma multiforme: exploratory radiogenomic analysis by using quantitative image features, Radiology 273 (1) (2014) 168–174.

[17] P. Prasanna, J. Patel, S. Partovi, A. Madabhushi, P. Tiwari, Radiomic features from the peritumoral brain parenchyma on treatment-naive multi-parametric MR imaging predict long versus short-term survival in glioblastoma multiforme: preliminary findings, Eur. Radiol. 27 (10) (2017) 4188–4197.

[18] S. Bae, Y.S. Choi, S.S. Ahn, J.H. Chang, S.G. Kang, E.H. Kim, S.H. Kim, S.K. Lee, Radiomic MRI phenotyping of glioblastoma: improving survival prediction, Radiology (2018) 180200.

[19] R.Y. Huang, R. Rahman, K.V. Ballman, S.J. Felten, S.K. Anderson, B.M. Ellingson, L. Nayak, E.Q. Lee, L.E. Abrey, E. Galanis, D.A. Reardon, W.B. Pope, T.F. Cloughesy, P.Y. Wen, The impact of T2/FLAIR evaluation per RANO criteria on response assessment of recurrent glioblastoma patients treated with bevacizumab, Clin. Cancer Res. 22 (3) (2016) 575–581.

[20] W.B. Pope, J. Sayre, A. Perlina, J.P. Villablanca, P.S. Mischel, T.F. Cloughesy, MR imaging correlates of survival in patients with high-grade gliomas, AJNR Am. J. Neuroradiol. 26 (10) (2005) 2466–2474.

[21] M.A. Hammoud, R. Sawaya, W. Shi, P.F. Thall, N.E. Leeds, Prognostic significance of preoperative MRI scans in glioblastoma multiforme, J. Neurooncol. 27 (1) (1996) 65–73.

[22] K. Clark, B. Vendt, K. Smith, J. Freymann, J. Kirby, P. Koppel, S. Moore, S. Phillips, D. Maffitt, M. Pringle, L. Tarbox, F. Prior, The Cancer Imaging Archive (TCIA): maintaining and operating a public information repository, J. Digit. Imaging 26 (6) (2013) 1045–1057.

[23] J.J.M. van Griethuysen, A. Fedorov, C. Parmar, A. Hosny, N. Aucoin, V. Narayan, R.G.H. Beets-Tan, J.C. Fillion-Robin, S. Pieper, H.J.W.L. Aerts, Computational radiomics system to decode the radiographic phenotype, Cancer Res. 77 (21) (2017) E104–E107.

[24] H. Ishwaran, U.B. Kogalur, E.H. Blackstone, M.S. Lauer, Random survival forests, Ann. Appl. Stat. 2 (3) (2008) 841–860.

[25] H. Ishwaran, U.B. Kogalur, E.Z. Gorodeski, A.J. Minn, M.S. Lauer, High-dimensional

variable selection for survival data, J. Am. Stat. Assoc. 105 (489) (2010) 205–217.
[26] M. Kuhn, Building predictive models in r using the caret package, J. Stat. Softw. 28 (5) (2008) 1–26.
[27] F.E. Harrell Jr., R.M. Califf, D.B. Pryor, K.L. Lee, R.A. Rosati, Evaluating the yield of medical tests, JAMA 247 (18) (1982) 2543–2546.
[28] E.W. Steyerberg, A.J. Vickers, N.R. Cook, T. Gerds, M. Gonen, N. Obuchowski, M.J. Pencina, M.W. Kattan, Assessing the performance of prediction models: a framework for traditional and novel measures, Epidemiology 21 (1) (2010) 128–138.
[29] Y. Benjamini, Y. Hochberg, Controlling the false discovery rate: a practical and powerful approach to multiple testing, journal of the royal statistical society, Ser. B (Methodological) 57 (1) (1995) 289–300.
[30] M.M. Inda, R. Bonavia, A. Mukasa, Y. Narita, D.W. Sah, S. Vandenberg, C. Brennan, T.G. Johns, R. Bachoo, P. Hadwiger, P. Tan, R.A. Depinho, W. Cavenee, F. Furnari, Tumor heterogeneity is an active process maintained by a mutant EGFR-induced cytokine circuit in glioblastoma, Genes Dev. 24 (16) (2010) 1731–1745.
[31] J.M. Lemee, A. Clavreul, P. Menei, Intratumoral heterogeneity in glioblastoma: don't forget the peritumoral brain zone, Neuro Oncol. 17 (10) (2015) 1322–1332.
[32] J.M. Lemee, A. Clavreul, M. Aubry, E. Com, M. de Tayrac, P.A. Eliat, C. Henry, A. Rousseau, J. Mosser, P. Menei, Characterizing the peritumoral brain zone in glioblastoma: a multidisciplinary analysis, J. Neurooncol. 122 (1) (2015) 53–61.
[33] M.M. Binabaj, A. Bahrami, S. ShahidSales, M. Joodi, M. Joudi Mashhad, S.M. Hassanian, K. Anvari, A. Avan, The prognostic value of MGMT promoter methylation in glioblastoma: a meta-analysis of clinical trials, J. Cell. Physiol. 233 (1) (2018) 378–386.
[34] T.J. Brown, M.C. Brennan, M. Li, E.W. Church, N.J. Brandmeir, K.L. Rakszawski, A.S. Patel, E.B. Rizk, D. Suki, R. Sawaya, M. Glantz, Association of the extent of resection with survival in glioblastoma: a systematic review and meta-analysis, JAMA Oncol. 2 (11) (2016) 1460–1469.
[35] M.B. Khan, S. Chakraborty, J.A. Boockvar, Gross total resection of glioblastoma improves overall survival and progression-free survival compared to subtotal resection or biopsy alone, Neurosurgery 79 (6) (2016) N12–n13.
[36] C. Henker, T. Kriesen, Ä. Glass, B. Schneider, Jürgen Piek, Volumetric quantification of glioblastoma: experiences with different measurement techniques and impact on survival, J. Neurooncol. 135 (2) (2017) 391–402.
[37] S.Y. Liu, W.Z. Mei, Z.X. Lin, Pre-operative peritumoral edema and survival rate in glioblastoma multiforme, Oncol. Res. Treat. 36 (11) (2013) 679–684.
[38] A. Chaddad, C. Desrosiers, M. Toews, Radiomic analysis of multi-contrast brain MRI for the prediction of survival in patients with glioblastoma multiforme, Conf. Proc. IEEE Eng. Med. Biol. Soc. 2016 (2016) 4035–4038.